Copper- and Silver-Containing Monolithic Silica-Supported Preparations for Selective Propene−Propane Adsorption from the Gas Phase

M. Kargol,[†,‡] J. Zajac,*[,†] D. J. Jones,[†] J. Rozière,[†] Th. Steriotis,[§] A. Jiménez-López,[||] and E. Rodríguez-Castellón[||]

Laboratoire des Agrégats Moléculaires et Matériaux Inorganiques, UMR 5072, Université Montpellier 2, Place E. Bataillon, 34095 Montpellier Cedex 5, France, Institute of Physical Chemistry, National Center for Scientific Research "DEMOKRITOS", Aghia Paraskevi, 153-10, Athens, Greece, and Departamento de Química Inorgánica, Cristalografía y Mineralogía, Facultad de Ciencias, Unidad Asociada del Instituto de Catálisis y Petroleoquímica, CSIC, Universidad de Málaga, Campus de Teatinos, 29071 Málaga, Spain

Received May 26, 2005. Revised Manuscript Received August 11, 2005

Cylindrically shaped macroscopic-in-size bodies of aluminum-doped silica possessing uniformly sized mesopores have been used as supports for copper- and silver-based formulations in the selective adsorption of propene against propane in the gas phase. The metal addition was achieved using $AgNO_3$ or $Cu(NO_3)_2$ in aqueous solution by either postsynthesis incipient wetness impregnation or direct incorporation in the synthesis stage, the overall metal content in samples being 2, 5, 10, and 20 wt %. The effect of metal addition on the degree of Al insertion into the silica matrix was evaluated by ^{27}Al magic-angle spinning NMR. The nature of surface metal species was studied by X-ray photoelectron spectroscopy and temperature-programmed reduction by H_2. Individual adsorption of propene and propane was measured at room temperature, and the selectivity coefficient was calculated as a function of the pressure and molar fraction of propene in the binary gas mixture. Within the series of Cu-derivatized adsorbents, the equilibrium selectivity is a complex function of the nature, amount, and dispersion degree of the copper species available on the surface. Contrary to expectations, both Cu(I) and Cu(II) states may give good propene−propane selectivity performance. For Ag-containing adsorbents the selectivity is mainly related to the nature and distribution of the silver species exposed on the surface, showing little dependence upon the overall Ag(I) content. The shaped sample functionalized with only 5 wt % of silver in the synthesis stage (*Ag5*SiAl20) appears to be the best monolithic adsorbent since it combines good selectivity performance (selectivity ratio of 37) and high specific surface area (ca. 900 $m^2\ g^{-1}$). Compared to fine-particle porous materials previously reported in the literature, the monolithic adsorbent form is more useful for industrial uses.

Introduction

Selective adsorption from the gas phase is an alternate approach to distillation for the separation of alkene−alkane mixtures. Progress in the preparation of solid adsorbents possessing appropriate adsorptive characteristics, such as selectivity, capacity, rate, and reversibility, has allowed the development of cyclic adsorption−desorption processes involving solid−gas systems. Pressure/vacuum swing adsorption (PSA-VSA) principles constitute the basis for an efficient separation process in which the adsorbent bed is cycled from adsorption to desorption by changing the pressure inside the adsorber.[1] Here the solid−gas system is not far from attaining adsorption equilibrium, and a very selective adsorbent is needed if alkene of high purity is to be recovered in the blow-down step. Sulfonic acid resins, silica gel, γ-Al_2O_3, zeolites, pillared clays, and ordered mesoporous silica, used alone or as high-surface-area supports for dispersing transition-metal cations in π-complexation adsorbents, have been reported to selectively adsorb light alkenes against their saturated counterparts.[2−13] Järvelin and Fair also proposed a three-step breakthrough procedure for propene−

* Corresponding author. E-mail: zajac@univ-montp2.fr.
[†] Université Montpellier 2.
[‡] Permanent address: Institute of Chemical Engineering, Polish Academy of Sciences, Baltycka 5, 44-100 Gliwice, Poland.
[§] National Center for Scientific Research "DEMOKRITOS.
[||] Universidad de Málaga.

(1) Jasra, R. V.; Choudary, N. V.; Bhat, Th. S. G. *Sep. Sci. Technol.* **1991**, *27*, 885.
(2) Yang, R. T.; Kikkinides, E. S. *AIChE J.* **1995**, *41*, 509.
(3) Chen, J. P.; Yang, R. T. *Langmuir* **1995**, *11*, 3450.
(4) Cheng, L. S.; Yang, R. T. *Adsorption* **1995**, *1*, 61.
(5) Chen, N.; Yang, R. T. *Ind. Eng. Chem. Res.* **1996**, *35*, 4020.
(6) Rege, S. U.; Padin, J.; Yang, R. T. *AIChE J* **1998**, *44*, 799.
(7) Huang, H. Y.; Padin, J.; Yang, R. T. *J. Phys. Chem. B* **1999**, *103*, 3206.
(8) Huang, H. Y.; Padin, J.; Yang, R. T. *Ind. Eng. Chem. Res.* **1999**, *38*, 2720.
(9) Padin, J.; Yang, R. T. *Chem. Eng. Sci.* **2000**, *55*, 2607.
(10) Newalkar, B. L.; Choudary, N. V.; Kumar, P.; Komarneni, S.; Bhat, Th. S. G. *Chem. Mater.* **2002**, *14*, 304.
(11) Newalkar, B. L.; Choudary, N. V.; Turaga, U. T.; Vijayalakshmi, R. P.; Kumar, P.; Komarneni, S.; Bhat, Th. S. G. *Chem. Mater.* **2003**, *15*, 1474.
(12) Grande, C. A.; Araujo, J. D. P.; Firpo, N.; Basaldella, E.; Rodrigues, A. E. *Langmuir* **2004**, *20*, 5291.
(13) Kargol, M.; Zajac, J.; Jones, D. J.; Steriotis, Th.; Rozière, J.; Vitse, P. *Chem. Mater.* **2004**, *16*, 3911.

10.1021/cm051120e CCC: $30.25 © 2005 American Chemical Society
Published on Web 10/28/2005

propane separation from a gas mixture diluted with an inert gas using zeolite molecular sieves and activated carbon.[14] A relatively concentrated stream of propene can be removed during regeneration cycles by a variable-temperature stepwise desorption and without the use of diluents.

In any industrial implementation of alkene−alkane separation the structural and surface properties of the adsorbent should be modeled according to the specific cost and operational conditions. The commercial use of microporous adsorbents in cyclic adsorption−desorption processes is limited by low reversibility and slow diffusion effects at ambient temperatures and by the risk of coke deposition over the solid surface or alkene polymerization when higher process temperatures are applied.[6,15−17] New process designs for adsorptive separation can take advantage of the promising results obtained with copper- or silver-functionalized adsorbents.[2,3,5,7−9,12,13] π-Complexation bonding of alkene molecules to the surface active sites is stronger than that induced by van der Waals forces alone, leading to high adsorption selectivity and capacity for the unsaturated gas component. At the same time π bonds between alkenes and transition-metal ions are weak enough to be broken during simple engineering operations such as raising the temperature or decreasing the pressure in the system.[18] Several materials preparation variables including the synthesis route and the method of metal addition were shown to affect selective adsorption of alkenes.[2,9,12,13]

The external form and size of the adsorbent preparations is another factor to be taken into consideration in the process design. To limit the pressure drop over the adsorbent bed use of powdered samples is excluded, and particulate adsorbents or monolithic structures are more suitable.

Ordered mesoporous silica possessing large internal surface area and high porosity with controllable and narrowly distributed pore sizes prepared by surfactant-assisted synthesis are promising candidates for adsorbate supports.[9,12,13] Numerous reactive Si−OH groups on which to underlie chemical modification of the surface and the possibility of incorporating various heteroatoms into the silica framework[19,20] may result in a wide range of modified products. Silica materials containing transition metals can be prepared by a variety of methods,[9,12,13,21−23] among which incipient wetness impregnation is a standard technique used by industry in adsorbent and catalyst preparation. With the direct liquid crystal templating (DLCT) pathway in high-concentration surfactant solutions[24−26] the nanostructure of the resulting macroscopic monolith, a cast of the parent liquid-crystalline phase, is dictated only to a limited extent by the reagents and synthesis conditions so that the adsorbent can be easily formulated for a particular application already in the synthesis stage without any further costly treatment.

The intention of the present study was to prepare monolithic silica-supported adsorbents having high selectivity and capacity for alkene−alkane adsorption in the form suitable for industrial use. In our previous report[13] copper- and silver-functionalized adsorbents supported on cylindrically shaped macroscopic-in-size silica bodies with a regular pore network were synthesized via the DLCT method using commercially available nonionic surfactants as templates. The metal addition was achieved by ion exchange with an appropriate metal nitrate in aqueous solution on the moulded and calcined substrates to yield porous adsorbents containing highly dispersed Ag(I) and Cu(II) cations. The ion-exchange capacity of the materials was enhanced by doping the silica framework with various amounts of aluminum. High adsorption selectivity of propene over propane at low alkene concentrations in the gaseous mixture was predicted from measurements of the individual adsorption of both components. It was ascribed to chemisorption of the unsaturated hydrocarbon molecules on surface sites due to the presence of the transition metal. Since cuprous salts are not water soluble a Cu(I)-functionalized adsorbent was obtained by a partial reduction of a Cu(II)-exchanged precursor in the sorption apparatus and the adsorption tests were performed immediately after reduction to avoid the disproportionation of Cu(I) to Cu(II) and metallic copper. The following trend of the metal cation effect was obtained for the equilibrium selectivity on the derivatized adsorbents: $Ag^+ > Cu^+ > Cu^{2+}$. The amount of Al in the framework appeared to have little effect on propene−propane selectivity.

To complete the previous work cylindrically shaped adsorbents functionalized with different amounts of copper or silver were prepared using incipient wetness impregnation and direct incorporation as methods of copper and silver addition from aqueous solution of $AgNO_3$ or $Cu(NO_3)_2$. Two series of aluminosilicates derivatized with different amounts of metal were obtained. The suitability of the prepared adsorbent formulations for selective alkene−alkane adsorption was assessed on the basis of the individual adsorption of propene and propane from the gas phase. The nature and content of silver and copper species is shown to be very important in optimizing the propene−propane selectivity.

Experimental Section

Chemicals. Tetraethyl orthosilicate (TEOS) and the nonionic poly(ethylene glycol) dodecyl ether surfactant Brij30 were purchased from Aldrich. Copper nitrate trihydrate, $Cu(NO_3)_2 \cdot 3H_2O$, and aluminum nitrate nonahydrate, $Al(NO_3)_3 \cdot 9H_2O$, were Merck products. Silver nitrate, $AgNO_3$, and a 0.1 M nitric acid solution were obtained from Fisher. Gaseous ammonia, nitrogen, helium, propane, and propene of high purity were supplied by Air Liquide.

(14) Järvelin, H.; Fair, J. R. *Ind. Eng. Chem. Res.* **1993**, *32*, 2201.
(15) Da Silva, F. A.; Rodrigues, A. E. *Ind. Eng. Chem. Res.* **1999**, *38*, 2051.
(16) Peterson, D. L.; Helfferich, F.; Griep, R. K. *Soc. Chem. Ind., London* **1968**, 217.
(17) Boucheffa, Y.; Thomazeau, C.; Cartraud, P.; Magnoux, P.; Guisnet, M.; Jullian, S. *Ind. Eng. Chem. Res.* **1997**, *36*, 3198.
(18) Humphrey, J. L.; Keller, G. E., II *Separation Process Technology*; McGraw-Hill: New York, 1997.
(19) Chen, L. Y.; Jaenicke, S.; Chuah, G. K. *Microporous Mater.* **1997**, *12*, 323.
(20) Tuel, A. *Microporous Mesporous Mater.* **1999**, *27*, 151.
(21) Ziolek, M.; Sobczak, I.; Decyk, P.; Nowak, I. *Stud. Sci. Catal.* **1999**, *125*, 633.
(22) Hartman, M. *Stud. Sci. Catal.* **2000**, *128*, 215.
(23) Miller, J. T.; Schreier, M.; Kropf, A. J.; Regalbuto, J. R. *J. Catal.* **2004**, *225*, 203.
(24) Göltner, C. G.; Antonietti, M. *Adv. Mater.* **1997**, *9*, 431.
(25) Tolbert, S. H.; Firouzi, A.; Stucky, G. D.; Chmelka, B. F. *Science* **1997**, *278*, 264.
(26) Rozière, J.; Brandhorst, M.; Dutartre, R.; Jacquin, M.; Jones, D. J.; Vitse, P.; Zajac, J. *J. Mater. Chem.* **2001**, *11*, 3254.

Adsorbent Preparation. The typical synthesis route used to prepare the shaped aluminosilicates following the direct liquid-crystal templating pathway in high-concentration surfactant solution and acidic medium is detailed in ref 13. The mass ratio of water: Brij30:TEOS was 1:1:3. Aluminum nitrate was added as the last reagent to a homogeneous mixture of dilute HNO_3, Brij30, and TEOS. The Si:Al molar ratio was 20, and the resulting material is further designated SiAl20. Cylindrically shaped SiAl20 was made in appropriate glass moulds, aged for several days, and calcined at 833 K for 6 h under a flow of air. The resulting crack-free cylinders of ca. 2 mm in diameter and 3−5 mm in length were subsequently derivatized with varying amounts of copper and silver by incipient wetness impregnation using aqueous solutions. The desired amount of $Cu(NO_3)_2$ or $AgNO_3$ was dissolved in sufficient water just to fill the pore volume of the support. A solid sample of 0.5 g was first dried overnight at 373 K, immersed in the previously prepared solution, and then placed in a tightly sealed glass vial. The impregnation stage was carried out at room temperature for 2 days. Afterward, the impregnated sample was dried at 373 K. The functionalized aluminosilicates are referred to as Si*MX*, where *M* denotes the added metal (*M* = Cu or Ag) and *X* is the metal content in the final sample (wt %).

Subsequently, cylindrically shaped SiAl20 were prepared by direct incorporation of copper or silver in the initial synthesis stage through addition of the desired amounts of $Cu(NO_3)_2 \cdot 3H_2O$ or $AgNO_3$ salts, stirring first with TEOS for 5 min and then with dilute HNO_3 for about 30 min to obtain a transparent solution. Brij30 was added afterward and the mixture again stirred for 10 min before introducing $Al(NO_3)_3 \cdot 9H_2O$. The postsynthesis treatment, moulding, and calcination were performed following the operating procedures described previously. Depending on the type (*M*) and amount (*X*) of incorporated metal, the aluminosilicates of this category are designated *MX*SiAl20. The copper or silver content *X* in a sample was varied between 2 and 20 wt %.

Adsorbent Characterization. Solid-state ^{27}Al NMR spectra were recorded at 104.3 MHz using a Bruker ASX400 spectrometer. Measurements of nitrogen gas adsorption onto cylindrically shaped samples at 77 K were carried out with the aid of a volumetric Analsorb 9011 apparatus developed in house. Prior to adsorption experiments samples were outgassed overnight down to 10^{-3} Torr at 493 K. Determination of parameters describing the 'average' pore network, i.e., the mesopore specific surface area, S_{mes}, the mesopore and micropore volumes, V_{mes} and V_{mic}, and the mesopore diameter, d_p, was based on the improved MP method.[26] X-ray photoelectron spectroscopy (XPS) analysis was carried out with a Physical Electronics PHI 5700 instrument equipped with a Mg Kα X-ray excitation source (300 W, 15 kV, 1253.6 eV) and a hemispherical electron analyzer. The spectra of cylindrically shaped samples (ca. 150 mg) were recorded in the constant pass energy mode at 29.35 eV using a 720 μm diameter analysis area. PHI ACCESS ESCA-V6.0 F software was used for acquisition and analysis of data. Binding energies (BE) were referenced to the C 1s line at 284.8 eV and determined with resolution as good as 0.1 eV. A Shirley-type background was subtracted from the signals. The recorded spectra were fitted assuming Gaussian−Lorentzian peak shape so as to determine the binding energy of the various element core levels. Temperature-programmed reduction (TPR) measurements were performed utilizing a Micromeritics AutoChem 2910. A weighed amount (ca. 150 mg) of the sample was held in a quartz reactor. The vapor impurities were removed by flowing helium over the sample at a flow rate of 30 mL min^{-1} at 523 K for 2 h, and then the system was cooled to room temperature. Reduction of the adsorbent was carried out from room temperature to 923 K using a heating rate of 5 K min^{-1}. During TPR runs a mixture of 10 vol % hydrogen and 90 vol % helium was passing through the system at a flow rate of 50 mL min^{-1}. The change in hydrogen concentration was monitored continuously with a thermal conductivity detector (TCD). Any H_2O produced during the reduction of the adsorbent was trapped using a dry ice trap.

Hydrocarbon Adsorption Measurements and Selectivity Determination. The individual adsorption of propane and propene from the gas phase at 298 K was studied using a Micromeritics ASAP 2010 apparatus. A solid sample of ca. 150 mg was placed in a glass cell and outgassed overnight at 523 K. Then it was cooled to 298 K in a flow of helium. During adsorption measurements successive doses of the reactive gas (propene or propane) were sent onto the sample until a given equilibrium pressure was reached. The amount adsorbed was determined after each adsorption step. The adsorption procedure was continued up to an equilibrium pressure of 760 Torr. The individual adsorption isotherms of propane and propene under static conditions were subsequently used to calculate the equilibrium selectivity of propene toward propane from the following equation[13]

$$S_{21} = \frac{\Gamma_2(1-X_2)}{\Gamma_1 X_2} \tag{1}$$

where X_2 is the mole fraction of propene in the hypothetical mixture of propane(1) and propene (2) and Γ_j (j = 1, 2) is the amount adsorbed of a given component from a single gas phase.

Results

In laboratory-scale adsorbent preparation it is important to optimize the amount of aluminum incorporated in the silica framework. On one hand, framework-substituted silica presents improved thermal and hydrothermal stability compared to the purely siliceous material.[19] On the other hand, materials rich in aluminum possess broader pores and their internal nanostructure is less well ordered. In the context of the present application, the presence of 'extraframework' aluminum that provides Lewis-type acidity in various aluminosilicates should be also mentioned.[13] Padin and Yang[9] showed that a transfer of electron density from the silver ions to the Lewis-acid sites at the surface of alumina weakened the π-complexation bonds with alkenes and that pure silica provided a better substrate due to the lack of coordinatively unsaturated Al^{3+} ions. With the aluminosilicates studied in the present work the Si:Al molar ratio in the shaped adsorbents was adjusted to 20 so as to maximize the proportion of silicon substituted by aluminum in the walls of the mesoporous silica.

The dispersion of copper or silver over the surface of SiAl20 by incipient wetness impregnation appears to have no effect on the degree of Al incorporation. The impregnated samples contain some 'extraframework' aluminum (mostly octahedrally coordinated), as in the pristine substrate.[13] For the materials derivatized during synthesis the effect of copper or silver addition is illustrated by ^{27}Al MAS NMR spectra in Figure 1. The NMR spectra of the calcined samples all present an intense resonance at δ 52 ppm arising from tetrahedrally coordinated aluminum and a second line at δ 0 ppm from six-coordinate aluminum noticeable only for low copper and silver loadings. As the amount of transition-metal added to the aluminosilicate framework increases, the first signal becomes somewhat broader and more intense whereas

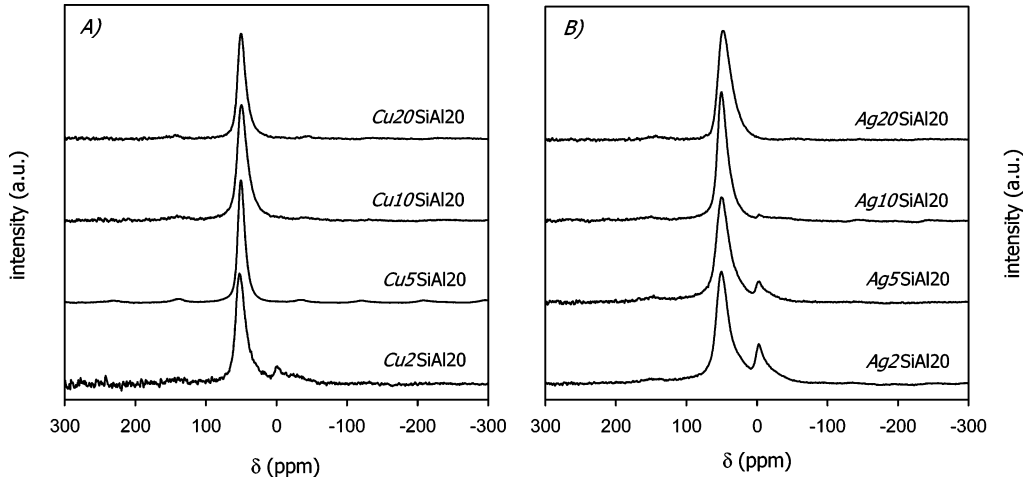

Figure 1. ^{27}Al MAS NMR spectra of cylindrically shaped aluminosilicates prepared with a Si:Al ratio of 20 and functionalized with copper and silver by direct incorporation in the synthesis stage.

Table 1. Specific Surface Area (S_{BET}), Mesopore Surface Area (S_{mes}), Mesopore (V_{mes}) and Micropore (V_{mic}) Volumes, and Mean Mesopore Diameter (d_p) of the Shaped Aluminosilicates Derivatized with Cu(II) and Ag(I) by Impregnation and Drying

sample	S_{BET} ($m^2\,g^{-1}$)	S_{mes} ($m^2\,g^{-1}$)	V_{mes} ($cm^3\,g^{-1}$)	d_p (nm)	V_{mic} ($cm^3\,g^{-1}$)
SiAl20	911	639	0.38	2.4	0.07
SiAl20*Cu2*	848	595	0.38	2.6	0.05
SiAl20*Cu5*	871	564	0.41	2.9	0.07
SiAl20*Cu10*	489	277	0.21	3.0	0.05
SiAl20*Cu20*	454	260	0.18	2.7	0.04
SiAl20*Ag2*	917	678	0.41	2.4	0.05
SiAl20*Ag5*	927	670	0.46	2.7	0.05
SiAl20*Ag10*	603	404	0.24	2.4	0.05
SiAl20*Ag20*	577	355	0.23	2.6	0.05

Table 2. Specific Surface Area (S_{BET}), Mesopore Surface Area (S_{mes}), Mesopore (V_{mes}) and *M*icropore (V_{mic}) Volumes, and Mean Mesopore Diameter (d_p) of the Shaped Aluminosilicates Derivatized with Cu(II) and Ag(I) by Direct Incorporation in the Synthesis Stage

sample	S_{BET} ($m^2\,g^{-1}$)	S_{mes} ($m^2\,g^{-1}$)	V_{mes} ($cm^3\,g^{-1}$)	d_p (nm)	V_{mic} ($cm^3\,g^{-1}$)
*Cu2*SiAl20	784	536	0.30	2.2	0.08
*Cu5*SiAl20	813	547	0.31	2.3	0.07
*Cu10*SiAl20	960	819	0.44	2.2	0.03
*Cu20*SiAl20	875	670	0.46	2.7	0.03
*Ag2*SiAl20	909	633	0.34	2.1	0.07
*Ag5*SiAl20	890	632	0.34	2.2	0.07
*Ag10*SiAl20	841	584	0.32	2.2	0.07
*Ag20*SiAl20	585	424	0.25	2.4	0.05

the relative intensity of the second signal diminishes. Therefore, extraframework Al is progressively transferred into either the framework or highly disordered, NMR-silent environments. The disappearance of signal arising from octahedral Al with increasing transition-metal content is more pronounced in the case of copper. *Cu10*SiAl20 and *Cu20*SiAl20 seem to contain uniquely framework Al.

Surface Area and Pore Size of Functionalized Adsorbents. All isotherms (not shown here) of nitrogen gas adsorption at 77 K onto cylindrically shaped aluminosilicate bodies derivatized with Cu(II) and Ag(I) are characteristic of materials with small mesopores. The specific surface area and pore structure parameters of adsorbents obtained by impregnation and drying are given in Table 1, and those of samples prepared by direct incorporation in the synthesis stage are reported in Table 2. The surface parameters of the pristine material SiAl20, taken from ref 13, are included in Table 1 for comparison purposes.

Impregnation and drying of the shaped aluminosilicates cause their S_{BET}, S_{mes} and V_{mes} parameters to decrease and their d_p values to increase, the effects being more pronounced in the case of copper. When the transition-metal content does not exceed 5 wt %, small alterations are observed. For high metal loadings corresponding to 10 and 20 wt % of metal in the sample the surface parameters undergo significant modification during impregnation. A decrease in S_{BET} and consequent decrease in V_{mes} allow pore blockage by growing metal clusters to be postulated. The above changes should be interpreted with caution because of significant uncertainty in the surface parameters determination inherent in the adsorption model and evaluation method used. Some irregularity in the trends observed may be certainly ascribed to hydrolytically induced changes in the adsorbent porosity during the postsynthesis functionalization in addition to uncontrolled pore blockage. After all, these changes are still less pronounced than those induced by ion exchange, especially in the case of silver.[13]

In contrast, direct incorporation of Ag(I) or Cu(II) nitrate is accompanied by a small increase in the average pore diameter. For samples with high metal content this derivatization procedure better preserves the porosity compared to ion exchange and incipient wetness impregnation. For samples containing silver the S_{BET} value decreases with increasing metal content. The specific surface area of

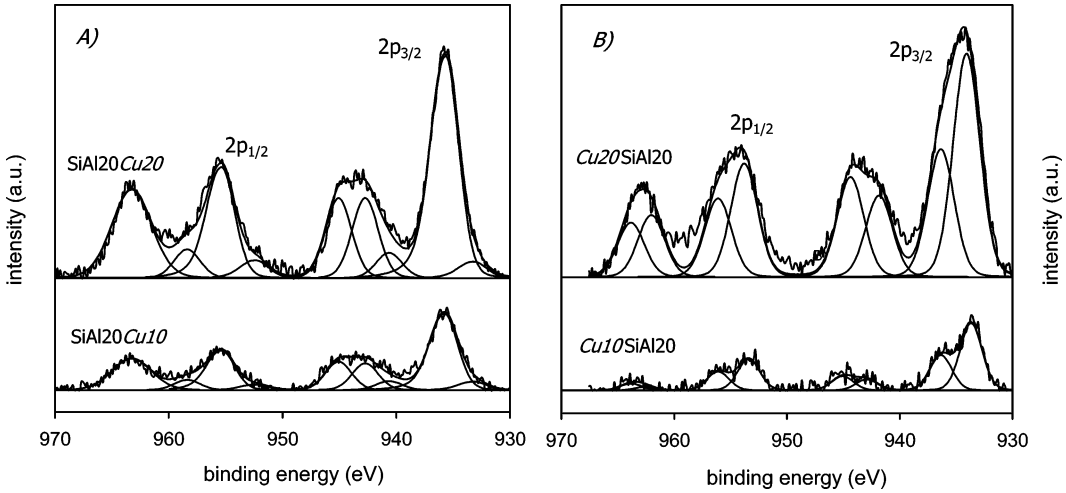

Figure 2. XPS spectra of Cu 2p core levels acquired from two shaped aluminosilicates with 10 and 20 wt % copper loadings and the corresponding curve fits obtained using Gaussian line shapes with a linear background: (A) Cu-impregnated adsorbents and (B) Cu-containing adsorbents prepared by direct synthesis.

*Ag20*SiAl20 is almost one-half that of the other samples, whereas the mean pore diameter is only a little greater. This adsorbent also has the smallest pore volume. It seems probable that a large proportion of active silver sites are within the pores, where they form bigger clusters with a concomitant decrease in the degree of dispersion and significant pore blockage. In the case of Cu(II)-derivatized materials the trends in S_{BET}, V_{mes}, and d_p with increasing metal content are less regular. For example, incorporation of 20 wt % of copper is possible without greatly compromising the large surface area, the high pore volume, and the small pore diameter. In consequence, pore blockage cannot really be deduced from the observed changes.

XPS. Characterization of the oxidation state of copper and silver in metal species present on the surface of the derivatized adsorbents may be made by means of X-ray photoelectron spectroscopy (XPS). Representative XPS spectra of the Cu 2p core regions acquired from Cu-containing samples loaded with 10 and 20 wt % of metal are presented in Figure 2. They are of low signal-to-noise ratio type as a consequence of a short acquisition time of 10 min used to examine the core level C 1s and Cu 2p regions in order to avoid, as much as possible, photoreduction of Cu(II) species. Large shake-up satellite peaks on the high binding energy side of the main photoelectron peaks are characteristic of the Cu(II) oxidation state. The appropriate curve fits are also shown in Figure 2.

For each of the impregnated samples the peak fit of the Cu $2p_{3/2}$ core level reveals two binding energy states. The peak positions and relative contributions from these features in the spectrum are collected in Table 3. The largest intensity peak components at 935.5−936.0 eV in the Cu $2p_{3/2}$ core region can be assigned to a dispersed Cu(II) state associated with nitrate species[27] possibly remaining on the surface after drying. This observation is in agreement with the blue-green color of the impregnated aluminosilicates, independent of the metal loading. Peaks at 933.2 or 933.5 eV are indicative of the presence of CuO at the surface, the corresponding binding energies being close to the 933.6 eV position observed in the XPS spectrum of 'bulk' copper oxide deposited on a thin SiO_2 film.[28] The relative contribution from this form of copper attains a maximum of 20% on the surface of SiAl20*Cu5*. Table 3 also summarizes some atomic contents in the near surface region of the impregnated samples calculated from the XPS peaks corresponding to the various elements and taking into account atomic sensitivity factors for all the orbitals scanned.

Table 3. Peak Fit of the XPS Cu $2p_{3/2}$ Core Level and Elemental Chemical Analysis in the near Surface Region of Cu-Impregnated Cylindrically Shaped Aluminosilicates

sample	SiAl20*Cu2*	SiAl20*Cu5*	SiAl20*Cu10*	SiAl20*Cu20*
Cu $2p_{3/2}$ BE (eV)	933.5 (15%)	933.2 (20%)	933.2 (10%)	933.2 (7%)
	935.8 (85%)	936.0 (80%)	935.8 (90%)	935.7 (93%)
Cu a.c. (%)	0.50	1.33	3.10	6.33
Si a.c. (%)	30.49	30.56	26.66	14.68
O a.c. (%)	69.05	67.98	69.58	76.12
Al a.c. (%)	*1.12*	*a*	*a*	*a*
Cu:Si atomic ratio	0.016	0.044	0.116	0.431

[a] No data available (overlapping of Al 2p and Cu $3p_{3/2}$ signals).

Table 4. Peak Fit of the XPS Cu $2p_{3/2}$ Core Level and Elemental Chemical Analysis in the near Surface Region of Cylindrically Shaped Aluminosilicates Derivatized with Copper by Direct Incorporation in the Synthesis Stage

sample	*Cu2*SiAl20	*Cu5*SiAl20	*Cu10*SiAl20	*Cu20*SiAl20
Cu $2p_{3/2}$ BE (eV)	933.9	933.7 (77%)	933.7 (64%)	933.7 (58%)
		936.5 (23%)	936.5 (36%)	936.5 (42%)
Cu a.c. (%)	0.19	0.57	1.01	4.37
Si a.c. (%)	30.67	30.13	30.06	27.73
O a.c. (%)	67.76	67.58	68.93	67.90
Al a.c. (%)	*1.38*	*1.12*	*a*	*a*
Cu:Si atomic ratio	0.006	0.019	0.034	0.158

[a] No data available (overlapping of Al 2p and Cu $3p_{3/2}$ signals).

Interpretation of the XPS spectra of aluminosilicates derivatized with copper by direct incorporation in the synthesis stage is more complicated. Examples of XPS scans are shown in Figure 2 B. The peak fit of the Cu $2p_{3/2}$ core level reveals two binding energy states, which are reported in Table 4 together with their relative contributions. In the case of

(27) Moreno-Tost, R.; Santamaría-González, J.; Maireles-Torres, P.; Rodríguez-Castellón, E.; Jiménez-López, A. *Catal. Lett.* **2002**, *82*, 205.

(28) Espinos, J. P.; Morales, J.; Barranco, A.; Caballero, A.; Holgado, J. P.; González-Elipe, A. R. *J. Phys. Chem. B* **2002**, *106*, 6921.

Table 5. Peak Fit of the XPS Ag $3d_{5/2}$ Core Level and Elemental Chemical Analysis in the near Surface Region of Ag-Impregnated Cylindrically Shaped Aluminosilicates

sample	SiAl20*Ag2*	SiAl20*Ag5*	SiAl20*Ag10*	SiAl20*Ag20*
Ag $3d_{5/2}$ BE (eV)	368.4 (82%) 369.5 (18%)	368.6	368.4	368.3
Ag a.c. (%)	0.68	2.48	4.30	6.64
Si a.c. (%)	29.64	27.66	26.67	24.71
O a.c. (%)	68.21	67.38	64.79	62.57
Al a.c. (%)	1.31	1.54	2.01	1.85
Ag:Si atomic ratio	0.023	0.090	0.161	0.269

Table 6. Peak Fit of the XPS Ag $3d_{5/2}$ Core Level and Elemental Chemical Analysis in the near Surface Region of Cylindrically Shaped Aluminosilicates Derivatized with Silver by Direct Incorporation in the Synthesis Stage

sample	*Ag2*SiAl20	*Ag5*SiAl20	*Ag10*SiAl20	*Ag20*SiAl20
Ag $3d_{5/2}$ BE (eV)	368.2 (77%) 369.3 (23%)	368.4 (82%) 369.6 (18%)	368.3 (87%) 369.5 (13%)	368.4
Ag a.c. (%)	0.36	0.57	1.29	2.99
Si a.c. (%)	29.32	29.54	29.58	29.82
O a.c. (%)	68.78	68.59	67.47	65.35
Al a.c. (%)	1.53	1.29	1.45	1.38
Ag:Si atomic ratio	0.012	0.019	0.044	0.100

*Cu2*SiAl20 curve fit of the XPS spectrum gives two peaks centered at about 933.9 and 953.3 eV for the Cu $2p_{3/2}$ and $2p_{1/2}$ core levels. Since no shake-up satellites are observed, the presence of a Cu(I) state is to be postulated. The feature at 933.7 eV also dominates in XPS scans of *Cu5*SiAl20 and *Cu10*SiAl20, which look very similar. Shake-up satellites appear in the XPS spectra of the Cu 2p core regions acquired from samples with copper loadings higher than 2 wt %, indicating the presence of Cu(II) species. A feature at 936.5 eV can be assigned to Cu(II) ions residing in the exchange sites at the adsorbent surface and coordinated to the surface oxygen.[29] The spectrum acquired from *Cu20*SiAl20 is quite different from the others since high satellite intensities can be seen within the 940−947 eV spectral region. It is noted that this sample was black at the beginning of the XPS measurements, and a preliminary XRD study revealed the presence of CuO crystallites, at least in the bulk of the solid. Thus, the peak at 933.7 eV can be here assigned to CuO, the concentration of which is higher than that corresponding to Cu(II) in the framework. In consequence, there are at least two different copper species on the surface of *Cu20*SiAl20 with intensities from Cu(II) largely dominating in the XPS scan. The elemental atomic contents in the near surface region of the above samples are given in Table 4.

In the case of aluminosilicates derivatized with silver use of XPS to identify the valence state of Ag is a delicate task because the theoretical binding energy values for Ag $3d_{5/2}$ with different oxidation states of silver are close, i.e., 368.2 and 367.7 eV for Ag(0) and Ag(I) states, respectively.[30] An acquisition time of 60 min was thus used to obtain clear XPS spectra that could be reliably processed. The binding energy states inferred from the peak fit of the Ag $3d_{5/2}$ core level for the eight samples are given in Tables 5 and 6. The major intensity is observed between 368.2 and 368.6 eV, depending on the sample studied. For aluminosilicates with a large amount of silver available on the surface this is the only peak that can be seen in XPS spectra within the Ag $3d_{5/2}$ spectral region. Even though the corresponding binding energies point to metallic silver, this peak is assigned to a dispersed Ag(I) state. One of the reasons is that XRD has not revealed the presence of any diffraction lines attributable to crystallites of metallic silver in SiAl20*Ag20*. Furthermore, the impregnated adsorbents were colorless, which is compatible with the presence of $AgNO_3$, whereas the slightly brown-black color of *Ag20*SiAl20 pointed out the existence of Ag_2O in this sample. It is known[28] that surface dispersion of deposited species and their interaction with the support may cause a marked increase in the corresponding binding energy monitored by XPS. An additional feature observed, for some samples, within the 369.3−396.6 eV Ag $3d_{5/2}$ region can be assigned to metallic Ag, appearing on the surface as a result of XPS-induced reduction of Ag(I) species. The intensity from Ag(0) is absent in XPS scans obtained with a short acquisition time, as illustrated in Figure 3. The results of the elemental chemical analysis are reported in Tables 5 and 6.

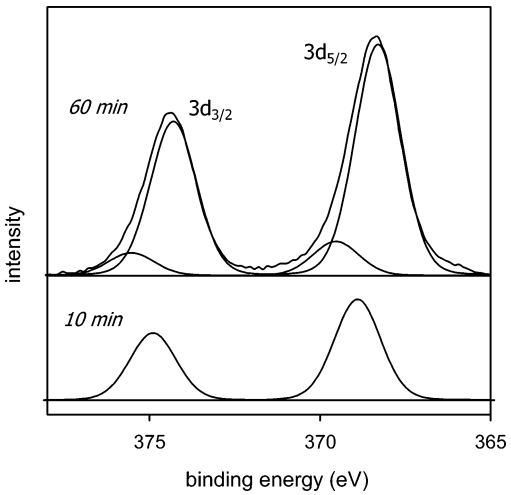

Figure 3. Influence of irradiation time on the XPS core-level Ag 3d spectrum of *Ag10*SiAl20.

TPR. Further information about the nature and distribution of the copper and silver species on the adsorbent surface can be obtained from H_2-TPR measurements.

Figure 4 illustrates the influence of metal loading on the normalized TPR profiles acquired from the surface of Cu-containing cylindrically shaped aluminosilicates. The normalized H_2 consumption was obtained by subtracting the original TPR signal from the baseline and dividing the result by the overall Cu content in a given sample. At first sight a single reduction process can be observed for each Cu-impregnated adsorbent in Figure 4A. The corresponding peak is large and asymmetric with the temperature of reduction maximum, T_m, attaining values in the range 475−495 K and increasing with copper loading. The height and width of the reduction peak also increase with increasing metal addition. Depending on the hydrogen concentration, flow rate, and heating rate a spread of T_m values (611−640 K) corresponding to reduction of the Cu(II) state to metallic copper is reported for samples of unsupported CuO obtained by nitrate calcination.[31,32] The value of T_m for a silica-supported CuO was found to be about 570 K.[32] Two maxima in the rate of hydrogen uptake obtained on Cu(II)-exchanged zeolites were

(29) Chaswick, D.; Hashemi, T. *Corros. Sci.* **1978**, *18*, 39.
(30) Sen, S.; Mahanty, S.; Roy, S.; Heintz, O.; Bourgeois, S.; Chaumont, D. *Thin Solid Films* **2005**, *474*, 245.

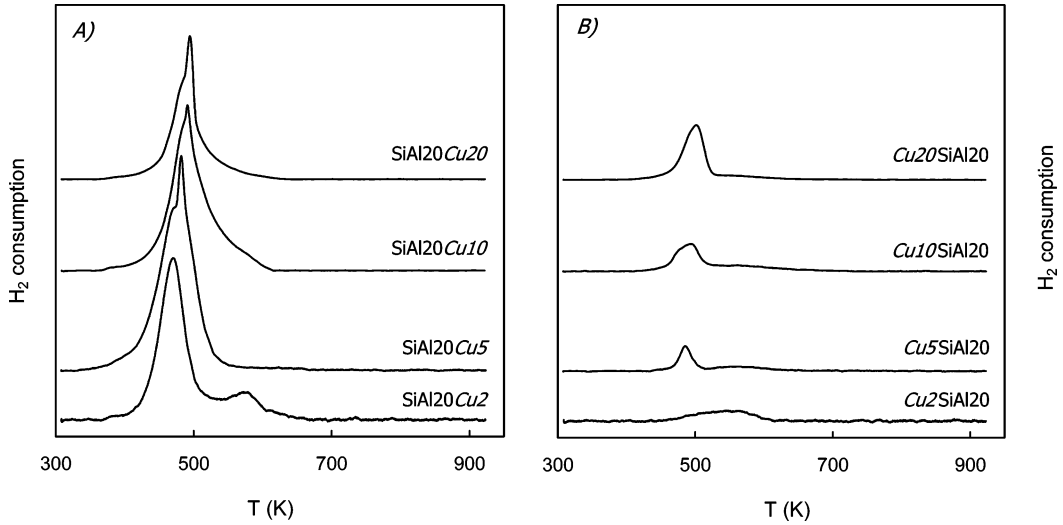

Figure 4. H_2-TPR profiles for the shaped aluminosilicates derivatized with copper by (A) impregnation and drying and (B) direct incorporation in the synthesis stage. The H_2-consumption scales are the same.

usually assigned as follows:[33] the first low-temperature maximum is due to reduction of CuO to Cu(0) and partial reduction of Cu(II) ions to Cu(I); the second maximum corresponds to reduction of Cu(I) species strongly interacting with the support. The one-step process observed in the present work is assigned to reduction of different Cu(II) species, like CuO and $Cu(NO_3)_2$, directly to metallic copper as no features in the H_2-TPR profiles are detected at high temperatures. Various aggregation states of the copper compounds present on the surface and their interactions with the support should result in different susceptibilities to reduction.[33,34] In the case of SiAl20*Cu2* the first low-temperature peak is followed by a second peak of weak intensity at the temperature region corresponding to that reported for reduction of supported CuO aggregates. The low-temperature feature may be thus assigned to reduction of better dispersed Cu(II) species. For two samples with the highest copper loading reduction occurs in a very broad *T* range (400−620 K). It may be that increasing the amount of $Cu(NO_3)_2$ deposited on the surface during impregnation results in complete loss of resolution of two reduction processes in the TPR profile and only one-step reduction is observed. The overall H_2 consumption per unit mass of copper, determined by integrating the normalized TPR profiles in Figure 4A, takes the following values: 6.2 s.u., SiAl20*Cu2*; 7.2 s.u., SiAl20*Cu5*; 6.1 s.u., SiAl20*Cu10*; 3.7 s.u., SiAl20*Cu20*. The smaller consumption value obtained for SiAl20*Cu20* suggests that only a part of the surface copper species is reduced in the TPR experiment.

The normalized H_2-TPR profiles acquired from the surface of Cu-derivatized adsorbents prepared by direct synthesis are shown in Figure 4B. For *Cu2*SiAl20 a broad reduction peak of low intensity is observed between 450 and 620 K with a maximum at ca. 560 K. The overall H_2 consumption is about one-tenth of that monitored for the impregnated homologue SiAl20*Cu2*. Since less copper is accessible at the surface of *Cu2*SiAl20 also, the above results are in agreement with the presence of surface Cu(I) species deduced from the XPS study. The TPR profiles of samples with a higher copper loading contain a single reduction peak, centered between 490 and 500 K, the intensity of which increases with increasing copper content. A shoulder of small intensity between 520 and 650 K accompanies each of these peaks, but this is not very visible in Figure 4B. The peak core corresponds to reduction of dispersed Cu(II) ions to metallic copper, whereas the shoulder likely represents a Cu(I) state. The overall H_2 consumption per unit mass of copper attains the following values: 0.7 s.u., *Cu5*SiAl20; 1.1 s.u., *Cu10*SiAl20; 1.5 s.u., *Cu20*SiAl20. This means that an important fraction of Cu(II) species is incorporated in the framework and thus not reducible.

Silver oxide Ag_2O and silver ions Ag^+ reduce more readily than their copper homologues. For example, reduction of Ag(I) ions to Ag(0) in zeolite Y was found to occur already at 393 K, whereas the lowest temperature of first major reduction maximum reported for Cu(II) in zeolites was 440 K.[35] The maximum reduction of bulk Ag_2O was ca. 420 K.[36] The normalized H_2-TPR profiles for aluminosilicates impregnated with $AgNO_3$ and dried are shown in Figure 5A. When the silver loading in the sample is greater than 2 wt %, the TPR curve is comprised of two unresolved peaks at ca. 380 and 410 K. The resulting composite peak results from reduction of Ag(I) species which differ in the degree of dispersion over the support. For example, the hydrogen consumption peak situated at lower temperature may correspond to reduction of Ag(I) to Ag(0) in dispersed Ag(I) species, whereas the second reduction contribution is probably due to the presence of bigger $AgNO_3$ particles on the surface of these samples. For SiAl20*Ag2* two distinct reduction peaks at 410 and 520 K can be seen. The appearance of the second contribution indicates that some Ag(I) ions interact with the support and thus are more

(31) Gentry, S. J.; Hurst, N. W.; Jones, A. *J. Chem. Soc., Faraday Trans. 1* **1981**, *77*, 603.
(32) Robertson, S. D.; McNicol, B. D.; De Baas, J. H.; Kloet, S. C.; Jenkins, J. W. *J. Catal.* **1975**, *37*, 424.
(33) Kieger, S.; Delahay, G.; Coq, B.; Neveu, B. *J. Catal.* **1999**, *183*, 267.
(34) Delahay, G.; Coq, B.; Broussous, L. *Appl. Catal. B* **1997**, *12*, 49.
(35) Uytterhoeven, J. B. *Acta Phys. Chem.* **1978**, *24*, 53.
(36) Dai, W.-L.; Cao, Y.; Ren, L.-P.; Yang, X.-L.; Xu, J.-H.; Li, H.-X.; He, H.-Y.; Fan, K.-N. *J. Catal.* **2004**, *229*, 80.

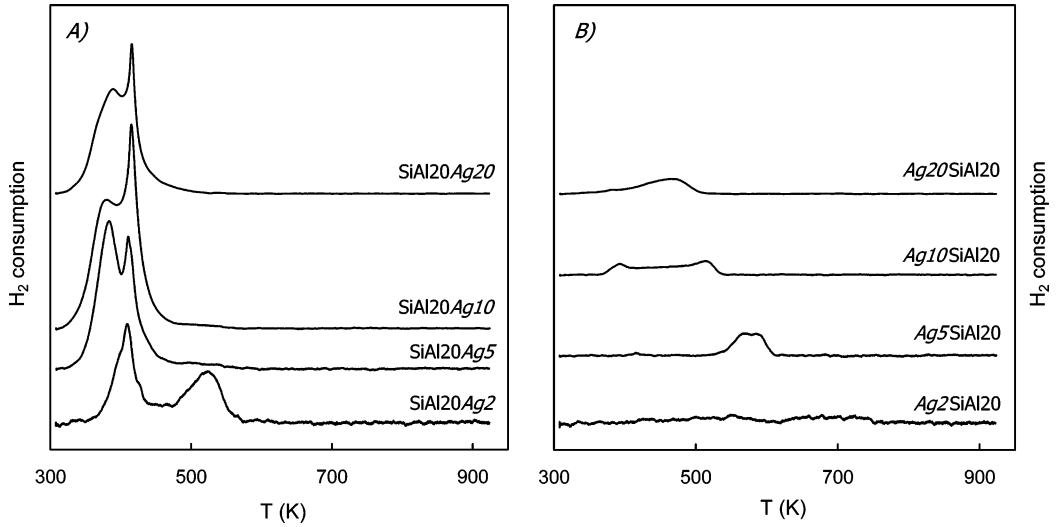

Figure 5. H_2-TPR profiles for the shaped aluminosilicates derivatized with silver by (A) impregnation and drying and (B) direct incorporation in the synthesis stage. The H_2-consumption scales are the same.

difficult to be reduced.[36] The overall H_2 consumption per unit mass of silver is as follows: 2.6 s.u., SiAl20*Ag2*; 3.4 s.u., SiAl20*Ag5*; 4.2 s.u., SiAl20*Ag10*; 3.0 s.u., SiAl20*Ag20*.

Ag-derivatized aluminosilicates prepared by direct synthesis provide H_2-TPR profiles composed of peaks of low intensity (Figure 5B). Here the overall hydrogen consumption is in excellent linear correlation with the total silver content; the H_2 consumption per unit mass of silver is ca. 0.5 s.u. for the four samples, clearly indicating that the majority of Ag(I) is located within the solid framework. Generally, the temperature of reduction maximum decreases with increasing silver loading, as already observed for $Ag-SiO_2-Al_2O_3$ sol−gel composites.[36] The T_m values are much higher than that of Ag_2O, suggesting that Ag(I) ions available on the surface interact strongly with the support. The broad reduction peaks in Figure 5B have complex shapes, meaning that surface silver species are very heterogeneous.

Propene and Propane Adsorption. Individual adsorption of propane and propene onto cylindrically shaped adsorbents was studied under static conditions at 298 K (the experimental curves are shown in the Supporting Information). The adsorption isotherms, $\Gamma = \Gamma(p)$, where Γ is the amount adsorbed at equilibrium pressure p, were of the Freundlich type for both gases.[13] The Freundlich isotherm equation was thus fitted to the experimental points, and the best-fit values of Freundlich constants, i.e., the preexponential factor k and the exponent n, are collected in Tables 7 and 8.

The exponent constant, n, in the Freundlich equation smaller than unity is commonly considered to reflect the energetic heterogeneity of active sites at the solid surface. The values of n reported in Tables 7 and 8 are much smaller than 1, especially for propene used as the adsorbate. Since the C_3H_6 adsorption curves are additionally quasi-vertical in the range of low equilibrium pressures, interactions of this gas with the surface active sites of the adsorbent should be particularly heterogeneous with a marked chemisorption component. In the case of propane the adsorption phenomenon seems to have a van der Waals character. For all samples studied the number of alkene molecules adsorbed at a given pressure is much greater than that of alkane, which

Table 7. Best-Fit Values of Freundlich Equation Constants and Ideal Selectivity at Selected Molar Fractions of Propene in the Propane(1)/Propene(2) Gas Mixture for the Shaped Aluminosilicates Derivatized with Copper and Silver by Impregnation and Drying

	Freundlich constants				equilibrium selectivity at a given X_2		
	propane(1)		propene(2)				
sample	k	n	k	n	0.05	0.5	0.7
SiAl20*Cu2*	0.010	0.73	0.145	0.38	13.1	1.8	1.2
SiAl20*Cu5*	0.007	0.77	0.104	0.42	12.1	1.9	1.4
SiAl20*Cu10*	0.005	0.77	0.052	0.48	9.6	1.8	1.3
SiAl20*Cu20*	0.007	0.67	0.159	0.24	21.3	1.8	1.2
SiAl20*Ag2*	0.016	0.68	0.235	0.32	16.3	1.8	1.2
SiAl20*Ag5*	0.015	0.68	0.346	0.26	21.7	2.0	1.3
SiAl20*Ag10*	0.013	0.67	0.170	0.37	16.9	2.2	1.4
SiAl20*Ag20*	0.016	0.68	0.403	0.25	22.7	2.0	1.3

Table 8. Best-Fit Values of Freundlich Equation Constants and Ideal Selectivity at Selected Molar Fractions of Propene in the Propane(1)/Propene(2) Gas Mixture for the Shaped Aluminosilicates Derivatized with Copper and Silver by Direct Incorporation in the Synthesis Stage

	Freundlich constants				equilibrium selectivity at a given X_2		
	propane(1)		propene(2)				
sample	k	n	k	n	0.05	0.5	0.7
*Cu2*SiAl20	0.009	0.76	0.023	0.74	5.5	2.3	1.8
*Cu5*SiAl20	0.010	0.73	0.026	0.68	5.6	1.8	1.4
*Cu10*SiAl20	0.013	0.72	0.164	0.38	12.3	1.6	1.1
*Cu20*SiAl20	0.011	0.71	0.100	0.44	11.0	1.7	1.2
*Ag2*SiAl20	0.014	0.72	0.250	0.35	15.9	1.9	1.3
*Ag5*SiAl20	0.015	0.56	0.198	0.35	36.6	4.1	2.5
*Ag10*SiAl20	0.021	0.64	0.247	0.31	15.7	1.6	1.1
*Ag20*SiAl20	0.015	0.61	0.242	0.25	23.0	2.0	1.2

means that the derivatized adsorbents are selective for propene against propane. The equilibrium selectivity ratios S_{21}, as calculated from the individual adsorption isotherms using eq 1, are reported in Tables 7 and 8 for three selected X_2 fractions of 0.05, 0.5, and 0.7. The differences among the samples are marked only at low molar fractions of propene in the gas mixture. No regular trends in the selectivity ratio at $X_2 = 0.05$ are observed with increasing metal loading. The nature and dispersion of metal species present on the adsorbent surface should be analyzed in this context. Ag-functionalized adsorbents are characterized by greater S_{21} values compared to the Cu-containing samples. The Cu-impregnated adsorbents exhibit somewhat higher

adsorption affinity for propene against propane than their homologues prepared by direct synthesis. In the case of samples derivatized with silver, no such differences can be really seen. *Ag5*SiAl20 appears to be the most efficient for selective adsorption of propene from gas mixtures containing small amounts of this component.

Discussion

Addition of copper or silver to the fine-pore cylindrical bodies is necessary for propene−propane adsorption to be selective under equilibrium conditions. The transition-metal insertion strategy via ion exchange from aqueous solution applied previously[13] to disperse metal species over cylindrically shaped aluminosilicates leads to intrinsic difficulty in achieving the desired exchange ratio and induces uncontrolled changes in the pore structure or even blockage of smaller pores by clustered Cu- or Ag-containing species. Better control of the metal loading is usually obtained using impregnation techniques. It should be, however, noted that the partially hydrophobic character of the surface of mesoporous aluminosilicates prepared by a surfactant-assisted synthesis and calcination[37] does not ensure proper wetting of the surface by aqueous solution and may diminish the dispersion degree of metal species.

The Cu(II) state associated with nitrate species is a major component of the Cu-impregnated adsorbents studied here, whereas the contribution from the minor CuO component decreases with increasing metal loading and never exceeds 20%. $AgNO_3$ is likely present in the Ag-derivatized samples. The Cu:Si or Ag:Si atomic surface ratio, as determined by XPS, is a perfect linear function of the overall transition-metal loading only for the first three members within each of the two derivatized series. For SiAl20*Cu20* a marked decrease in the Si atomic content is accompanied by an increase in the quantity of oxygen and copper atoms present in the near surface region (see Table 3). This means that the impregnating material $Cu(NO_3)_2$ forms on the surface extended zones of supermonolayer coverage, thereby masking the underlying silica matrix and diminishing the pore volume. Only the 'upper layer' of copper species is available to H_2 reduction under the TPR conditions, which explains why the overall H_2 consumption is much smaller compared to the three other samples of the series. When the overall metal loading is 10 or 20 wt % a significant decrease in the dispersion degree of the deposited phases, even leading to pore blockage, can be inferred from the conjunction of BET and TPR studies. Aggregation of copper or silver species on the surface of SiAl20*Cu20* and SiAl20*Ag20* does not make them less selective in propene−propane adsorption. On the contrary, these two samples exhibit the best selectivity within their homologous series, at least for small propene contents in the binary mixture with propane (see Table 7).

While postsynthesis insertion techniques can yield heterogeneous systems especially for large metal loadings, direct incorporation in the synthesis stage has been reported to represent a simpler and more reproducible way to disperse metal species into porous matrixes.[19,20] Nevertheless, when the active sites are located inside the walls they are inaccessible to guest molecules. Surface copper or silver species differ from those present in the impregnated adsorbents. For the Cu-derivatized samples with low and moderate metal loadings, most of the surface copper is in the Cu(I) oxidation state, usually considered as more appropriate for π-complexation of propene.[2−4] Cu(I) is probably obtained by reduction of Cu(II) during surfactant removal. When the overall copper content exceeds 2%, Cu(II) ions residing in the exchangeable sites at the adsorbent surface constitute the second type of copper species. *Cu20*SiAl20 contains mostly surface Cu(II) in the form of either exchangeable cations or CuO. The Ag-functionalized adsorbents most probably comprise Ag_2O in a variety of surface environments. Comparison of metal-to-silicon atomic ratios reported in Tables 4 and 6 with those obtained for the impregnated counterparts (Tables 3 and 5) allows estimating the percentage of metal exposed on the surface of the adsorbents derivatized during the synthesis: 37%, *Cu2*SiAl20; 43%, *Cu5*SiAl20; 30%, *Cu10*SiAl20; 37%, *Cu20*SiAl20; 52%, *Ag2*SiAl20; 21%, *Ag5*SiAl20; 27%, *Ag10*SiAl20; 37%, *Ag20*SiAl20. In most cases only one-third of the metal added to the reaction mixture is available on the surface of the derivatized adsorbents. The TPR results indicate better dispersion of surface species, and pore blockage is less pronounced than in the case of ion-exchanged or impregnated adsorbents.

The 'ideal' selectivity S_{21} calculated from eq 1 depends on two parameters: the molar fraction of propene X_2 and the pressure p. The profiles of S_{21} as a function of X_2 and p for the most selective samples within the four adsorbent series studied here are shown in Figure 6. These profiles have been generated from the Freundlich equation for the adsorption isotherm taking the best-fit values of k and n parameters collected in Tables 7 and 8. The main conclusion is that the selectivity ratio increases rapidly with decreasing X_2 fraction and slowly with decreasing pressure. The pressure dependence of S_{21}, even though not very marked, is of great importance in view of PSA-VSA applications of the functionalized adsorbents. The decrease in the selectivity with increasing propene content in the gas mixture should be a great disadvantage, but this requires comment. It should be noted that eq 1 is based on the assumption of ideal behavior of both gas components in the bulk and adsorbed phase. When the adsorption experiment is carried out under equilibrium conditions, this assumption implies the competitivity and additivity of solid−gas adsorption on active surface sites, which probably holds only for small X_2 fractions. The values of the ideal selectivity coefficient tend to unity with increasing mole fraction of propene in the bulk mixture, thereby giving the incorrect impression that the adsorption phenomenon becomes unselective. Propane can be only physisorbed at the solid−gas interface at any composition of the bulk phase. Thus, if the bulk propene activity is sufficiently high, the adsorbed layer should be mostly composed of chemisorbed and physisorbed alkene molecules. This would prevent further interaction between the propane and the adsorbent. In a PSA-VSA process any physisorbed portion of the adsorbate may be easily removed from the

(37) Meziani, M. J.; Zajac, J.; Douillard, J.-M.; Jones, D. J.; Partyka, S.; Rozière, J. *J. Colloid Interface Sci.* **2001**, *233*, 219.

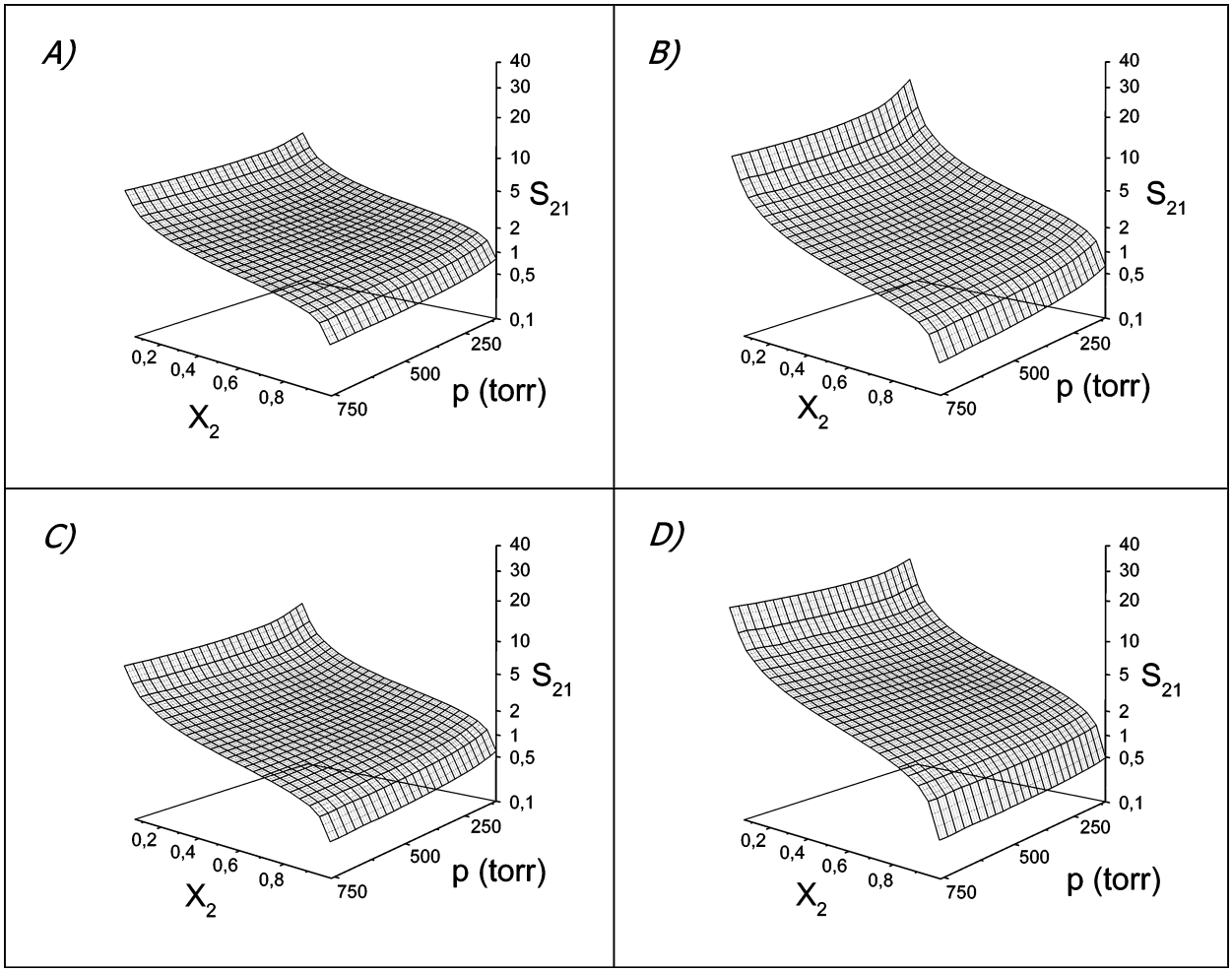

Figure 6. Ideal selectivity ratio S_{21} as a function of the pressure, p, and the molar fraction, X_2, of propene in the propane(1)/propene(2) gas mixture for the most selective samples within the four adsorbent series studied in the present paper: (A) SiAl20*Cu20*, (B) SiAl20*Ag20*, (C) *Cu10*SiAl20, and (D) *Ag5*SiAl20.

adsorbent, thereby leaving only pure propene in contact with the surface. Therefore, the actual selectivity ratio at high propene fractions X_2 should obviously be much higher than that calculated from eq 1.

In view of the equilibrium selectivity data at low X_2 fractions collected in Tables 7 and 8 or illustrated in Figure 6, Cu(II) surface species appear at least as efficient for the selective adsorption of alkenes as the Cu(I) state. The most selective among the Cu-impregnated adsorbents, SiAl20*Cu20* containing only Cu(II) species on the surface, has better selectivity performance than any of the samples derivatized with copper during the synthesis and any of the ion-exchanged adsorbents described previously.[13] Its selectivity coefficient of 21 is even higher than that of the sample ion exchanged with Cu(II) and subsequently reduced to Cu(I) prior to hydrocarbon adsorption measurements (it had a propene−propane selectivity ratio of 17[13]). Since the overall copper content in the latter sample is only one-third of that in SiAl20*Cu20*, the selectivity ratio clearly depends not only on the metal oxidation state but also on the overall copper quantity exposed on the surface. Impregnated samples contain more copper species in the near surface region, and thus, they are more selective than the adsorbents derivatized with the same amounts of metal during the synthesis. For the same copper oxidation state SiAl20*Cu20* is more selective than *Cu20*SiAl20, characterized by a lower density of surface copper and comprising both the exchangeable Cu(II) ions coordinated to the surface oxygen and the surface CuO. The effect of the counterion, i.e., O^{2-} for the adsorbents prepared by direct synthesis and NO_3^- in the impregnated samples, is thus another factor to be considered (the importance of this effect was underlined in ref 7). High dispersion of surface copper species appears to be less relevant to selective separation of propane−propene mixtures, although perhaps this parameter has not been sufficiently optimized in the present work.

For the adsorbents derivatized with silver the differences in the equilibrium selectivity between the two categories of adsorbent are less pronounced. The nature and dispersion degree of silver species seem to be crucial parameters. Despite lower metal content at the surface, the samples derivatized in the synthesis stage show selectivities comparable to those of their impregnated counterparts. The best propene−propane selectivity is achieved for *Ag5*SiAl20, which is thought to contain little Ag_2O highly dispersed on the surface and strongly interacting with the substrate (see TPR section). The amount of surface sites apparently has a secondary influence on the adsorbent performance in selective hydrocarbon adsorption. This trend is particularly pronounced in the case of Ag-impregnated materials. Here the distribution of surface $AgNO_3$ is postulated to have a heterogeneous, patchwise-like character, which prevents numerous propene molecules from chemical bonding with surface Ag(I) sites.

Selection of promising adsorbents for practical uses can be made on the basis of comparison among the impregnated and directly functionalized samples studied in the present paper and the ion-exchanged ones described previously.[13] The highest selectivity coefficient of 52 was obtained for an ion-exchanged SiAl20 sample loaded with 20% of silver. Nevertheless, poor repeatability of the ion-exchange procedure involving uncontrolled changes in the adsorbent porosity makes such adsorbents less attractive for industrial implementations of selective propene−propane adsorption. In the case of impregnated samples metal addition may be controlled to a greater extent but appropriate selectivity coefficients (attaining a value of 23 at the most) require high metal loadings. Insertion of large amounts of precious metal compounds increases the cost of adsorbent preparation. Furthermore, the decreased specific surface area of an ion-exchanged or impregnated sample with a high metal content results in a significant decrease in the propene adsorption capacity, thereby diminishing the amount of propene to be selectively removed from a gas mixture during one adsorption cycle. In this context, *Ag5*SiAl20 with a specific surface area of about 900 $m^2\ g^{-1}$ and a propene−propane selectivity ratio of 37 deserves to be considered as the best adsorbent. Direct incorporation of low percentages of silver is an attractive solution since it allows a significant cost reduction and good control of the adsorbent porosity.

Comparison of the evaluated selectivity and adsorption capacity parameters with the literature data is difficult since the hydrocarbon adsorption isotherms are often measured under different conditions for various alkane−alkene systems.[9−12] Furthermore, the quantities used to evaluate propene−propane selectivity are not always compatible. The performance of the best monolithic adsorbent is here compared with that of similar materials prepared in the form of powders, such as various ordered mesoporous silicas functionalized or not with Ag(I). For *Ag5*SiAl20 the propene adsorption capacity at 1 atm and 298 K is about 2.2 mmol g^{-1} and the propene−propane adsorption capacity ratio at the same pressure is equal to 5.5 (see Supporting Information). A similar propene adsorption value of 1.9 mmol g^{-1} was reported by Newalkar et al.[10] for ordered porous silica of the SBA-15 type at 1 atm and 303 K, but the best selectivity coefficient of this purely siliceous material was only about 8. The functionalized adsorbent prepared by incipient wetness impregnation of MCM-41 silica with $AgNO_3$ showed a maximum propene adsorption capacity of about 1.5 mmol g^{-1} at 343 K and a propene−propane adsorption capacity ratio of 4.5 at 1 atm.[9] Therefore, the selective performance of *Ag5*SiAl20 is still better, especially since increasing temperature diminishes mainly the physical adsorption contribution, thereby enhancing the capacity ratio. Grande and coworkers[12] announced high selectivity values up to about 45 at low propene pressures, as evaluated from the adsorbed phase concentrations for propene and propane at 343 K onto SBA-15 silica functionalized by incipient wetness impregnation with a considerable amount of $AgNO_3$ (Ag:Si weight ratio of 0.54). However, the specific surface area of this adsorbent was only 594 $m^2\ g^{-1}$, and it adsorbed much less propene per unit mass than *Ag5*SiAl20. The monolithic form of the prepared adsorbents gives them a significant advantage over fine-particle porous materials previously described in the literature. As an example, the pore structure may collapse during pressing or extruding the pristine powdered material in the industrial formulation of adsorbents. Therefore, the surface properties and observed trends reported for powders cannot necessarily be generalized to the adsorbents in their final form suitable for industrial use. The selectivity and adsorption capacity parameters included in the present paper hold for the cylindrically shaped macroscopic-in-size bodies functionalized with Cu(II), Cu(I), or Ag(I), which can be considered as adsorbent formulations attractive for industrial adsorbers exhibiting a low-pressure drop.

Conclusion

Cylindrically shaped mesoporous aluminosilicates moulded via the direct liquid-crystal templating procedure and functionalized with copper and silver by incipient wetness impregnation and direct incorporation in the synthesis stage have proved selective for adsorption of propene against propane under conditions favorable for the attainment of adsorption equilibrium. Compared to the ion-exchange procedure studied previously,[13] both metal addition methods described in the present work allow better control of the metal loading and pore structure. For the adsorbents derivatized with $Cu(NO_3)_2$ in aqueous medium the equilibrium selectivity is a complex function of the overall metal content in the sample as well as the oxidation state, nature, and dispersion degree of the copper species available on the surface. Unexpectedly, both Cu(I) and Cu(II) states appear capable of inducing good adsorbent performance. In the case of adsorbents functionalized with $AgNO_3$ the performance is closely related to the nature and distribution of metal species available on the surface, showing little dependence upon the overall Ag(I) content. Highly dispersed Ag_2O species, available on the surface of adsorbents functionalized in the synthesis stage with small amounts of silver nitrate, appear to be adequate for selective behavior as dispersed Ag(I) ions in ion-exchanged samples. From a practical viewpoint, *Ag5*SiAl20 with a specific surface area of about 900 $m^2\ g^{-1}$ and a propene−propane selectivity ratio of 37 appears to be the best monolithic adsorbent since direct incorporation of low percentages of silver contributes to a significant cost reduction in the adsorbent formulation. Compared to the fine-particle silica-based adsorbents reported in the literature, *Ag5*SiAl20 combines good propene−propane selectivity performance and high propene adsorption capacity whereas its monolithic form should be advantageous to industrial implementation of propene−propane separation.

Acknowledgment. Financial support from the European Growth Contract No. G5RD-CT-2001-00544 is acknowledged with thanks.

Supporting Information Available: Individual adsorption isotherms of propene and propane at 298 K on the cylindrically shaped aluminosilicates derivatized with copper or silver; for each type of addition method the isotherms are plotted on the same adsorption scale. This material is available free of charge via the Internet at http://pubs.acs.org.

CM051120E